J. Fluid Mech. (1982), *vol.* 125, *pp.* 203–218
Printed in Great Britain

Longitudinal-dispersion calculations in laminar flows by statistical analysis of molecular motions

By RAYMOND J. DEWEY† AND PAUL J. SULLIVAN
Department of Applied Mathematics, The University of Western Ontario, London, Ontario

(Received 22 November 1979 and in revised form 21 June 1982)

In this paper the streamwise growth of a passive contaminant cloud in the laminar flow within a uniform conduit is investigated. A probabilistic formulation, based on the Lagrangian motion of typical marked fluid molecules, is used to gain insight into the complex dispersion problem that exists at times that are significantly smaller (and often of more practical relevance) than those required for the asymptotic case discussed by Taylor (1953) to be valid.

Previous investigations of the small-time spread of a contaminant cloud in a tube by Lighthill (1966) and Chatwin (1976, 1977) were primarily concerned with a cloud near a tube axis as may be appropriate to an injection into the flow in arteries. When the contaminant is more uniformly spread over the conduit cross-section it is shown that, even at quite small times, the conduit boundary has a very pronounced influence on the streamwise contaminant distribution. Such a situation occurs, for example, when extracting sample fluid from a flow by means of a small-diameter sampling tube.

The streamwise spread of the contaminant cloud that results from an initial sheet of contaminant, spread uniformly over the conduit cross-section, is shown to depend critically on the Lagrangian mean-velocity history of a typical fluid molecule. This mean-velocity history function generally (and necessarily) is distinguished by a 'hump' whose location is determined by the proximity of the molecule's release position to the nearest conduit boundary. The 'hump' is a more-pronounced feature for release positions near a boundary than it is for contaminant molecules released near the conduit centre, where the 'hump' becomes almost indiscernible.

The specific case of flow between parallel plates is investigated using a random-walk model of the process. A significant difference is found from the results of an analysis that excludes the influence of the conduit boundaries on the streamwise contaminant distribution at times $t = O[d^4/\kappa U^2]^{\frac{1}{3}}$, where U is the mean-flow velocity, κ is the molecular diffusivity and d is the plate separation distance.

1. Introduction

A cloud of scalar contaminant is spread along the streamwise direction of the flow within a cylindrical conduit by both the direct contribution of mixing in the streamwise direction (diffusion) and the interaction of mixing in the cross-stream direction with the gradient of the streamwise velocity (dispersion). Although Taylor (1953) has shown that the contaminant cloud takes on a simple asymptotic shape (Gaussian with constant growth rate of variance), there are not many practical flows to which this analysis will apply (see Chatwin 1970, 1971; Sullivan 1971*b*; Dewey & Sullivan 1977).

† Permanent address: Gore & Storrie Ltd. Consulting Engineers, 1670 Bayview Ave., Toronto, Ontario M4G 3C2.

Model equations have been proposed to extend the work of Taylor (see Gill & Sankarasubramanian 1970; Smith 1981); however, the complexity of the contaminant dispersion problem at small times, as shown herein, suggests that correspondingly complex model equations may be required for an adequate representation (see Smith 1982). In this paper a direct probabilistic approach to the motion of marked fluid molecules (not unlike that of Chatwin 1977) is used to investigate the dispersion of a uniform contaminant sheet (normal in the flow direction) in a unidirectional laminar flow.

The small-time dispersion of a contaminant sheet has practical importance when one is extracting sample fluid from a flow by means of a small-diameter sampling tube, as for example in the use of a flow-through fluorometer (see Sullivan 1971*a*). Because of the smallness of the sampling-tube diameter (and the fact that the monitoring device integrates the sample-fluid property over the sample-tube cross-section) variations of concentration over the sample-tube cross-section are ignored. Streamwise mixing takes place during the small time interval in which the sample fluid passes from the inlet of the sampling tube to the monitoring instrument. The degree of resolution of the experimental procedure will depend upon the amount of streamwise mixing. For this problem one can, by superposition, replicate the dispersion from any one-dimensional contaminant-concentration signal using the solution for the dispersion of a thin uniform sheet of contaminant.

The two separate contributions to the streamwise spreading of a contaminant cloud, dispersion and streamwise diffusion, have a relative importance that depends on the time elapsed from release. At large time ($t\kappa/d^2 \gg 1$) the contribution of the streamwise diffusion is usually insignificant, as was first demonstrated by Taylor (1953). Following Taylor (1921) it is apparent that at extremely small times and away from the influence of the flow boundary the advective–diffusive interaction is unimportant. Lighthill (1966) and Chatwin (1976) considered the problem of a contaminant cloud released near the centre of a tube and before a significant amount of contaminant has had time to diffuse to the wall ($t\kappa/d^2 \ll 1$). Lighthill neglected the direct contribution of κ, which neglect was determined by Chatwin to be appropriate when $t\kappa/d^2 \gg (Ud/\kappa)^{-\frac{3}{2}}$. Smith (1982) has recently shown that, away from the conduit walls, the distribution of contaminant is essentially Gaussian at very small times. It is interesting that, as shown in Chatwin & Sullivan (1981), when there is a non-zero gradient of κ (unlike the present case) the contribution at small time due to the variability of κ will always become important before that due to the advective–diffusive interaction. The practical application cited in Lighthill (1966) and in Chatwin (1976) of an injection in large arteries may require a variable diffusivity when smaller blood vessels, in which the flow is thixotropic, is considered.

In this paper special consideration is given to the role of conduit boundaries in the streamwise spread of contaminant at small times. Even in a simple uniform flow there is a 'piling-up' of contaminant at the boundaries when a random-walk model is used (see Csanady 1973; Chandrasekhar 1943), and here one expects the zero-velocity condition at a solid boundary to have a significant effect on the streamwise contaminant distribution before too much time has elapsed. Chatwin (1977) has explored the case of the release of a contaminant sheet in a tube, and concludes that at extremely short times ($t\kappa/d^2 < 0{\cdot}01$) 'no significant contribution to the variance' comes from the region near the wall. This conclusion is not inconsistent with the findings of this paper in that here, in the flow between parallel plates, the effect of the wall is seen as a large tail on the distribution, which becomes more pronounced as time increases.

2. The dispersion of a contaminant sheet

In this section it will be shown how the dispersion of a contaminant sheet depends critically on the Lagrangian mean-velocity history of a fluid molecule. In the following section the behaviour of the mean-velocity history in general will be investigated, and specific calculations made for the flow between parallel plates.

The Lagrangian displacement vector $\mathbf{X}(t;\mathbf{X}(t_0))$ (with component $X_1(t;\mathbf{X}(t_0))$ in the streamwise direction) of a fluid molecule at time t on the condition of its release at $\mathbf{X}(t_0)$ at time t_0 is determined from

$$X_i(t;\mathbf{X}(t_0)) = \int_{t_0}^{t} v_i(t';\mathbf{X}(t_0))\,dt', \tag{1}$$

where $\mathbf{v}(t;\mathbf{X}(t_0))$ is the Lagrangian molecule velocity vector (component $v_1(t;\mathbf{X}(t_0))$ in the streamwise direction). Following Taylor (1921) the second moment of the streamwise displacement is found from

$$\frac{1}{2}\frac{d}{dt}\overline{X_1(t;\mathbf{X}(t_0))^2} = \int_{t_0}^{t} \overline{v_1(t;\mathbf{X}(t_0))\,v_1(t';\mathbf{X}(t_0))}\,dt', \tag{2}$$

where an overbar is used to denote an ensemble average. The velocity component $v_1(t;\mathbf{X}(t_0))$ depends on the release position $\mathbf{X}(t_0)$, and is non-stationary for small time intervals $t-t_0$. However, for sufficiently large $t-t_0$ the displacement $X_1(t;\mathbf{X}(t_0))-\overline{X_1(t;\mathbf{X}(t_0))}$ will be asymptotically Gaussian and the integral in (2) will become constant, as is discussed in Lumley (1972).

The Lagrangian streamwise velocity component can be written as

$$v_1(t;\mathbf{X}(t_0)) = u(X_2(t;\mathbf{X}(t_0)),\, X_3(t;\mathbf{X}(t_0))) + w_1', \tag{3}$$

where w_1' is the random microscopic streamwise velocity fluctuation due to thermal molecular activity, and is taken to be isotropic and uncorrelated with u and independent of space or time. $u(x_2, x_3)$ is the steady Eulerian streamwise velocity component of the flow;

$$\overline{w_1'} = 0. \tag{4}$$

Replacement of v_1 in (2) with (3) and the use of (4) leads to

$$\frac{1}{2}\frac{d}{dt}\overline{X_1(t;\mathbf{X}(t_0))^2} = \int_{t_0}^{t} \overline{u(X_2(t;\mathbf{X}(t_0)),\, X_3(t;\mathbf{X}(t_0)))\,u(X_2(t';\mathbf{X}(t_0)),\, X_3(t';\mathbf{X}(t_0)))}\,dt' + \kappa, \tag{5}$$

when $t-t_0 \gg t_1$, the integral timescale of w_1'. The result (5) is in essence the same as that derived by Saffman (1960) (see also Chatwin 1977), but with a different notation.

A very important simplification to (2), and hence to (5), results when an event in the ensemble is the release of a uniform sheet of marked molecules from a constant value of $X_1(t_0)$. In flows that are homogeneous in the streamwise direction there will be one corresponding path R where (see figure 1)

$$X_2(t_0) = a \rightarrow X_2(t;a,b) = a', \tag{6a}$$

$$X_3(t_0) = b \rightarrow X_3(t;a,b) = b' \tag{6b}$$

for every identical reverse path Q, where

$$X_2(t_0) = a' \rightarrow X_2(t;a',b') = a, \tag{7a}$$

$$X_3(t_0) = b' \rightarrow X_3(t;a',b') = b \tag{7b}$$

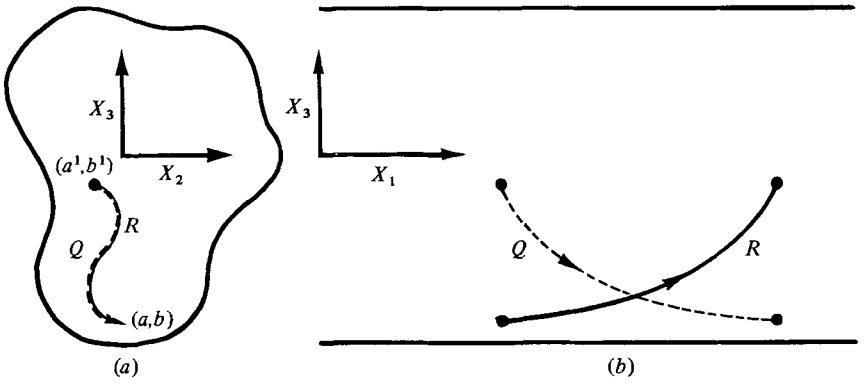

FIGURE 1. A definition sketch showing (*a*) an end view and (*b*) a cross-sectional side view of the conduit. Molecular paths R and Q are discussed in §2.

in the ensemble of events. As a consequence, the representation of (2) for a sheet release,

$$\frac{1}{2}\frac{d}{dt}\overline{X_1(t;X_1(t_0))^2} = \frac{1}{A}\iint_A dx_2\,dx_3 \int_{t_0}^{t} \overline{v_1(t;\mathbf{X}(t_0))\,v_1(t';\mathbf{X}(t_0))}\,dt', \tag{8}$$

where A is the conduit cross-sectional area, has the equivalent representation (by interchanging paths like Q with paths like R) as

$$\frac{1}{2}\frac{d}{dt}\overline{X_1(t;X_1(t_0))^2} = \frac{1}{A}\iint_A dx_2\,dx_3 \int_{t_0}^{t} \overline{v_1(t_0;\mathbf{X}(t_0))\,v_1(t';\mathbf{X}(t_0))}\,dt'. \tag{9}$$

In the notation of (5), (9) is

$$\frac{1}{2}\frac{d}{dt}\overline{X_1(t;X_1(t_0))^2} = \frac{1}{A}\iint_A dx_2\,dx_3 \int_{t_0}^{t} u(x_2,x_3)\,\overline{u(X_2(t';\mathbf{X}(t_0)),\,X_3(t';\mathbf{X}(t_0)))}\,dt' + \kappa. \tag{10}$$

Thus for the special case of the release of sheets of marked molecules the second moment is determined by the Lagrangian mean-velocity history

$$\overline{u(X_2(t';\mathbf{X}(t_0)),\,X_3(t';\mathbf{X}(t_0)))}$$

of molecules.† Equation (9) applies to both laminar and turbulent flows; however, further progress in turbulent-flow regimes requires assumptions that are outlined in Dewey & Sullivan (1979*a*) .

The mean-velocity history is determined from

$$\overline{u(X_2(t;\mathbf{X}(t_0)),\,X_3(t;\mathbf{X}(t_0)))} = \iint_A dx_2\,dx_3\,u(x_2,x_3)\,p(x_2,x_3,t-t_0;\mathbf{X}(t_0)), \tag{11}$$

where $p(x_2,x_3,t-t_0;\mathbf{X}(t_0))\,dx_2\,dx_3$ is the probability that a molecule released at location $\mathbf{X}(t_0)$ at time t_0 will be within x_2 and x_2+dx_2 and also x_3 and x_3+dx_3 at time

† A similar result to (10) can be derived for some time-dependent flows, and will be presented in a forthcoming paper.

t. The probability density function p is found from the solution of (see e.g. Chatwin 1977)

$$\frac{1}{\kappa}\frac{\partial p}{\partial t'} = \frac{\partial^2 p}{\partial x_2^2} + \frac{\partial^2 p}{\partial x_3^2}, \tag{12a}$$

$$t' = t - t_0, \tag{12b}$$

with $\partial p/\partial n = 0$ in the conduit boundary and

$$p(x_2, x_3, 0, \mathbf{X}(0)) = \delta(x_2 - X_2(0))\,\delta(x_3 - X_3(0)) \tag{12c}$$

such that

$$\lim_{t\to\infty} p = \frac{1}{A}, \tag{12d}$$

$$\iint_A dx_2\,dx_3\,p(x_2, x_3, t'; \mathbf{X}(0)) = 1. \tag{12e}$$

The solution to (12) can be written as an eigenvalue λ_n, eigenfunction $F_n(x_2, x_3; \mathbf{X}(0))$ expansion (see e.g. the discussion in Aris 1956):

$$p(x_2, x_3, t'; \mathbf{X}(0)) = \frac{1}{A} + \sum_{n=1}^{\infty} e^{-\lambda_n t'} F_n(x_2, x_3; \mathbf{X}(0)), \tag{13}$$

where for $t' \gg 1$

$$p \sim \frac{1}{A} + e^{-\lambda_1 t'} F_1(x_2, x_3; \mathbf{X}(0)). \tag{14}$$

Using (14) in (11) leads to

$$\bar{u} \sim U + \phi(\mathbf{X}(0))\, e^{-\lambda_1 t'}, \tag{15}$$

where

$$\phi(\mathbf{X}(0)) = \iint_A u(x_2, x_3)\, F_1(x_2, x_3; \mathbf{X}(0))\, dx_2\, dx_3. \tag{16}$$

Equation (15) suggests that the mean-velocity history approaches the flow-discharge velocity U in a regular exponential manner for large $t - t_0$. When (15) is used in (10) there results

$$\frac{1}{2}\frac{d\overline{X^2}}{dt} \sim U^2 t' + \psi(1 - e^{-\lambda_1 t'}) + \kappa, \tag{17}$$

where the constant ψ is given by

$$\psi = \frac{\lambda_1}{A} \iint_A u(x_2, x_3)\, \phi(x_2, x_3)\, dx_2\, dx_3. \tag{18}$$

It readily follows from (11) and (12) that for a sheet release the average displacement is

$$\overline{X}(t; X_1(t_0)) = U(t - t_0), \tag{19}$$

so that (17) can be written in terms of the variance as

$$\frac{1}{2}\frac{d}{dt}\overline{(X - \overline{X})^2} \sim \phi(1 - e^{-\lambda_1 t'}), \tag{20}$$

when the normally very small contribution due to the molecular diffusivity κ has been disregarded. The form of (20) is just that found for a tube by Chatwin (1977), for a rectangular conduit by Chatwin & Sullivan (1982), and for the flow between parallel plates by Dewey & Sullivan (1979*a*). In fact, to a good approximation, the form given in (20) was measured in a turbulent open-channel flow and discussed in Sullivan (1971*b*).

3. The mean-velocity history at small time

The simple monotonic approach of the mean-velocity history to the discharge velocity at large times shown in (15) cannot in general describe the small-time behaviour of a fluid molecule. Consider release positions (x_1', x_2') on the flow cross-section defined by

$$u(x_1', x_2') = U. \tag{21}$$

The mean-velocity history of such molecules begins and ends as the discharge velocity U. However, the ensemble-average displacement, $\overline{X_2(t; \mathbf{X}(t_0))}$ and $\overline{X_3(t; \mathbf{X}(t_0))}$ of these molecules begins at x_2' and x_3' and asymptotically approaches the centre of area of the cross-section, thereby resulting in interim values of the mean-velocity history that are different from the discharge velocity. It is to be noted that $\overline{X_2(t; \mathbf{X}(t_0))}$ and $\overline{X_3(t; \mathbf{X}(t_0))}$ do not change from the initial value at t_0 until molecules encounter the nearest solid boundary. It is only through the encounter of molecules with the solid boundary that the 'humps' on $\overline{u(X_2(t; \mathbf{X}(t_0)), X_3(t; \mathbf{X}(t_0)))}$ appear. The resulting 'hump' in the mean-velocity history is a quite general phenomenon and will occur in all flows, both laminar and turbulent, for which the location of the discharge velocity (as determined in (21)) is not coincident with the centre of area of the flow cross-section. It is only in flows like Couette flow when the position (x_1', x_2') is coincident with the centre of area (mid-distance between the plates) that a simple monotonic approach of the mean-velocity history to the discharge velocity will occur for release positions near (x_1', x_2').

As a specific example consider the laminar flow between parallel plates. The mean-velocity profile

$$u(y) = 6U\left(\frac{y}{d} - \left(\frac{y}{d}\right)^2\right) \tag{22}$$

over the flow depth $0 \leqslant y \leqslant d$ results in the mean-velocity history, for molecules released at position $Y(0)$ at $t = 0$,

$$\overline{u(Y(t);\, Y(0))} = U - \frac{6U}{\pi^2} \sum_{n=1}^{\infty} \frac{1}{n^2} \exp\left(-\left(\frac{2n\pi}{d}\right)^2 \kappa t\right) \cos\left(\frac{2n\pi}{d} Y(0)\right), \tag{23}$$

where

$$\overline{u(Y(t);\, Y(0))} = \int_0^d u(y)\, p(y, t;\, Y(0))\, dy, \tag{24}$$

$$p(y, t;\, Y(0)) = \frac{1}{d} \sum_{n=-\infty}^{\infty} \exp\left(-\left(\frac{n\pi}{d}\right)^2 \kappa t\right) \exp\left(\frac{n\pi}{d} iy\right) \cos\left(\frac{n\pi}{d} Y(0)\right) \tag{25}$$

have been used in (11) and (12) (see Dewey & Sullivan 1979*a*).

The form of the small-time behaviour of the Lagrangian mean-velocity history $\overline{u(Y(t);\, Y(0))}$ is not directly apparent from (23); however, it can readily be observed that†

$$\Omega_\tau = \Omega_{\xi\xi}, \tag{26}$$

with $\Omega(\tau, 0) = \Omega_\xi(\tau, \frac{1}{2}) = 0$, is satisfied by $\Omega(t;\, Y(0)) = [\bar{u}(Y(t);\, Y(0)) - U]/U$, $\tau = t\kappa/d^2$ and $\xi = Y(0)/d$. The solution to (26) is

$$\Omega(\tau, \xi) = (6\xi - 6\xi^2 - 1) - 12\tau + \mathscr{L}^{-1}\left[\frac{6\cosh\left((\tfrac{1}{2} - \xi)\, S^{\frac{1}{2}}\right)}{(S^3)^{\frac{1}{2}} \sinh\left(\tfrac{1}{2} S^{\frac{1}{2}}\right)}\right] \tag{27}$$

$$\Omega_\tau(\tau, \xi) = -12 + \mathscr{L}^{-1}\left[6\cosh\frac{\left((\tfrac{1}{2} - x)\, S^{\frac{1}{2}}\right)}{S^{\frac{1}{2}} \sinh\left(\tfrac{1}{2} S^{\frac{1}{2}}\right)}\right] \tag{28}$$

† This is indeed a very general result and (as pointed out by a referee) can be seen to result directly in, upon multiplication of 12(*a*) by $u(x_2, x_3)$ and integration over the cross-section, $\bar{u}_\tau = 6U(p(0, \tau;\, Y(0)) + p(1, \tau;\, Y(0))) - 12U$ for this specific parallel-plate case.

where $\mathscr{L}^{-1}$ denotes the inverse Laplace transform. As $S \to \infty$ (that is $\tau \to 0$)

$$\Omega_\tau(\tau, \xi) \sim -12 + \frac{6}{(\pi\tau)^{\frac{1}{2}}}\left(\exp\left(\frac{-\xi^2}{4\tau}\right) + \exp\left(-\frac{(1-\xi)^2}{4\tau}\right)\right). \tag{29}$$

When $\tau \to 0$, $\xi \neq 0$ and $\xi \neq 1$, it is clear from (29) that $\Omega(\tau, \xi)$ is everywhere decreasing. Of course $\Omega(\tau, \xi)$ cannot decrease everywhere, since this would lead to a decelerating flow. There is an increasingly thick layer, comprising release positions starting at $\xi = 0$, $\tau = 0$, for which the second term on the right-hand side of (29) is greater than 12. Molecules that started in this layer have increasing values of $\Omega(\tau, \xi)$ and balance all of the remaining release positions at larger values of ξ where $\Omega(\tau, \xi)$ is decreasing. This Lagrangian view of the mean velocity of fluid molecules is quite different from that observed when one looks at an array of hydrogen bubbles, for example, when the bubbles simply follow the Eulerian velocity profile.

As a result of the above, molecules released from positions with a mean velocity in excess of the discharge velocity U can have a mean-velocity history that diminishes below the value of U before ultimately returning to it. Also, molecules released from positions with a mean velocity below U can initially attain Lagrangian-mean velocities that are further removed from U before ultimately returning to U. This phenomenon is seen clearly on figures 2 (*a*–*c*).

The location of the 'hump' in the Lagrangian-mean-velocity-history curves can be found from a consideration of release positions near $\xi = 0$, where from (29)

$$\Omega_\tau(\tau, \xi) \sim -12 + \frac{6}{(\pi\tau)^{\frac{1}{2}}} \exp\left(\frac{-\xi^2}{4\tau}\right) = 0 \tag{30}$$

results in

$$\xi^2 = -4\tau \ln (2(\pi\tau)^{\frac{1}{2}}). \tag{31}$$

Figure 3 shows the typical value of $\Omega(\tau, 0{\cdot}16)$, with a straight line of slope -12 accurately describing the $\tau \to 0$ behaviour. This initial behaviour is found to be accurately true for all of the release positions $Y(0)$ shown on figures 2 (*a*–*c*). The modal values of $\Omega(\tau, \xi)$ shown as open circles on figures 2 (*a*–*c*) are transferred to figure 4, where they are shown to be in good agreement with the values given by (31).

For all release positions, excluding $\xi = 0$ and $\xi = 1$, there is an initial linear decrease in the mean-velocity history (i.e. $\Omega(\tau, \xi) = -12\tau + \Omega(0, \xi)$). The transition between this initial linear behaviour and the exponential decay to the discharge velocity at large times of (15) is marked by a 'hump' in the mean-velocity-history record that is located by (31) for release positions near the wall. It would appear from figures 2 (*a*–*c*) and figure 4 that 'humps' in the mean-velocity history for release positions $\frac{1}{4} < \xi < \frac{1}{2}$ are not discernible, and may occur at larger times than those for which the asymptotic expansion (29) remains valid.

4. The wall effect on dispersion at small times

In this section the direct contribution to the streamwise dispersion process at small times from the presence of a solid boundary will be assessed both with regard to when and how it affects the form of the cross-sectionally integrated contaminant concentration curve $\overline{C}(x, t)$.

A direct and simple approach that has met with considerable success elsewhere (see Bugliarello & Jackson 1964; Dewey & Sullivan 1979*a*, *b*; Chatwin & Sullivan 1982) is to use a random-walk model of a molecule's motion on the flow cross-section.† Here the actual process is simulated by matching the value of 2κ to the product of a

† Also referred to in a more general context as a Monte Carlo method.

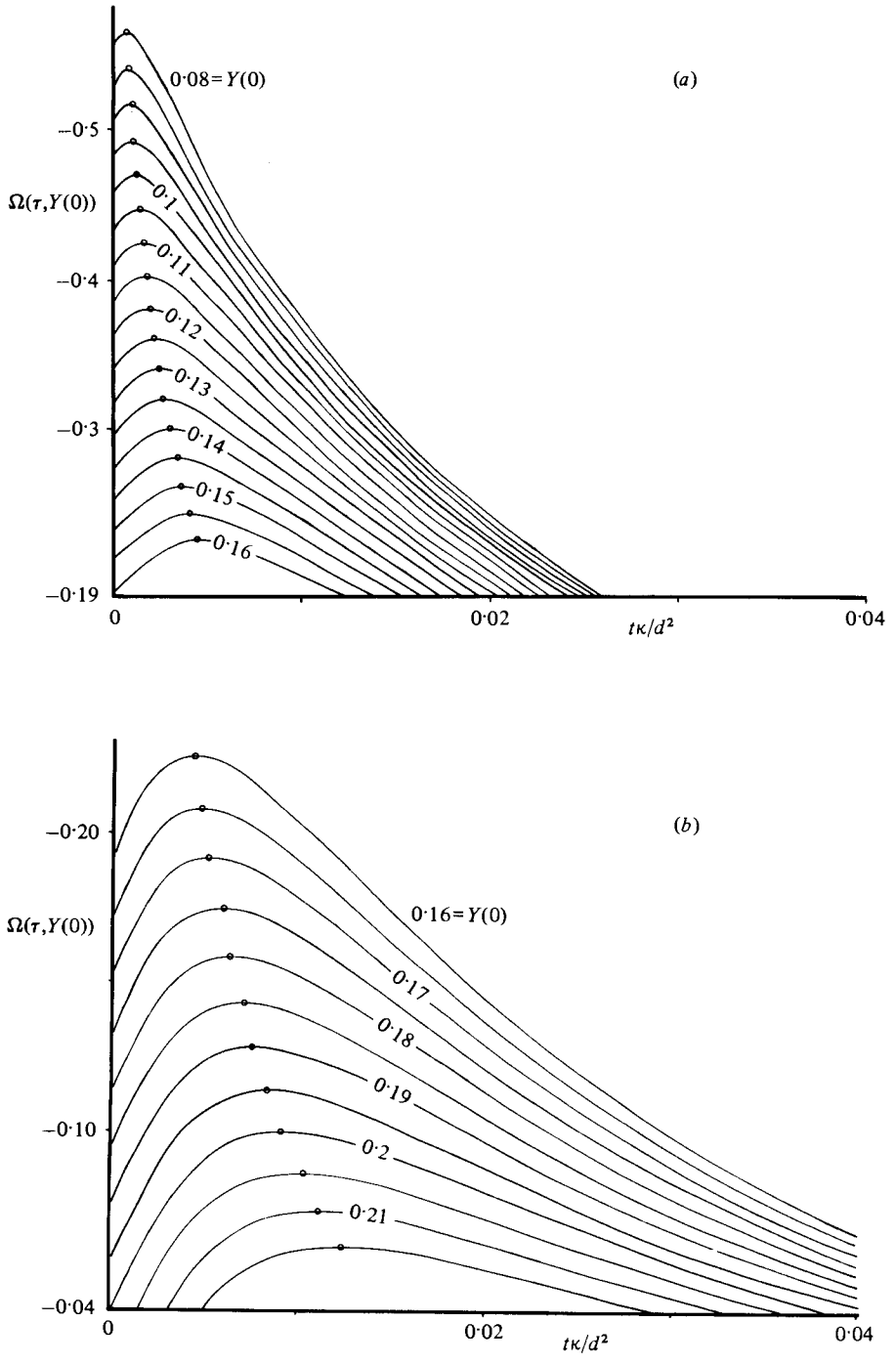

FIGURE 2(*a*, *b*). For caption see facing page.

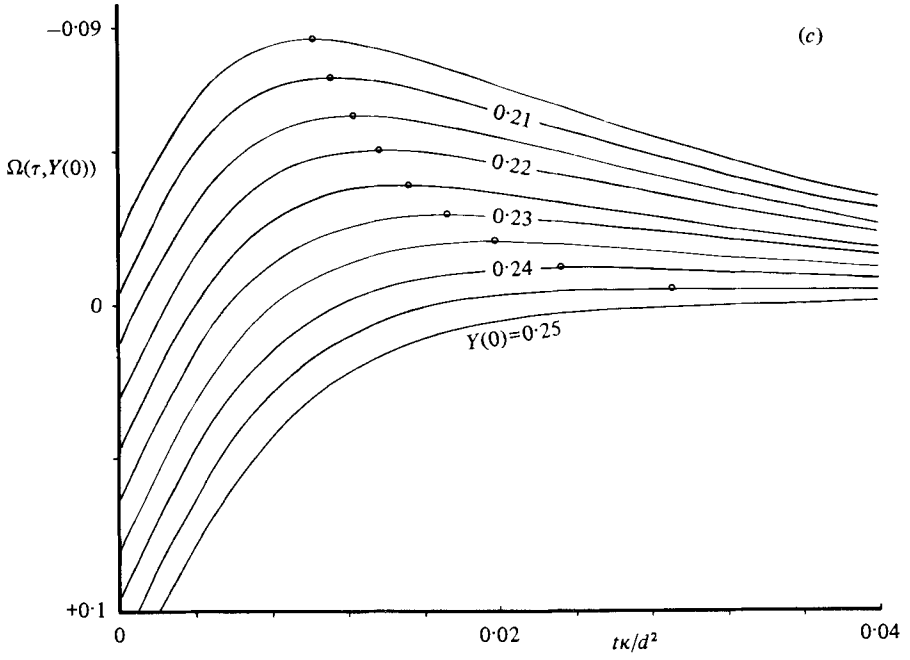

FIGURE 2. $\Omega(\tau, Y(0))$ versus $t\kappa/d^2$: ——, equation (23); ○, modal value.

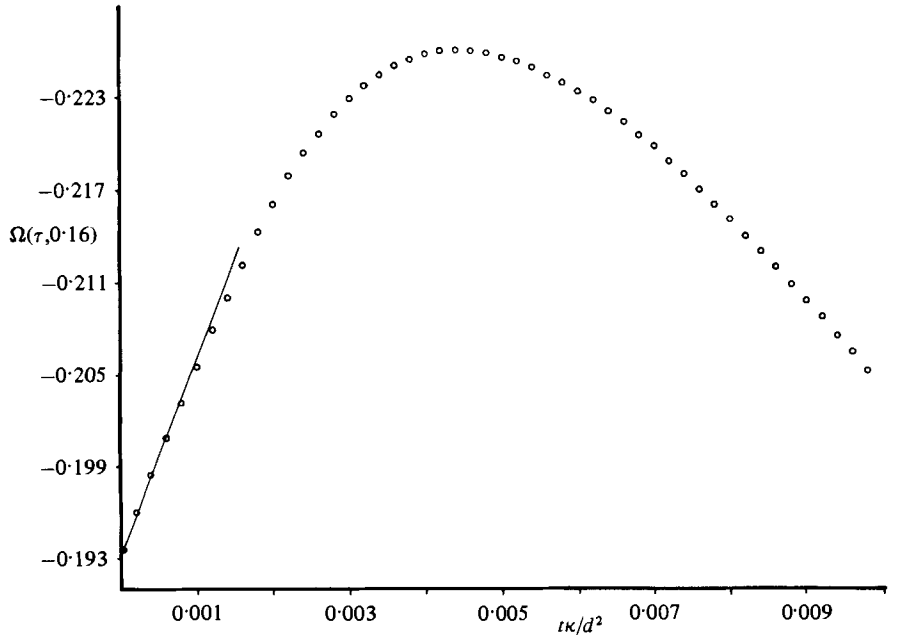

FIGURE 3. $\Omega(\tau, 0{\cdot}16)$ versus $t\kappa/d^2$: ——, -12 slope; ○, equation (23).

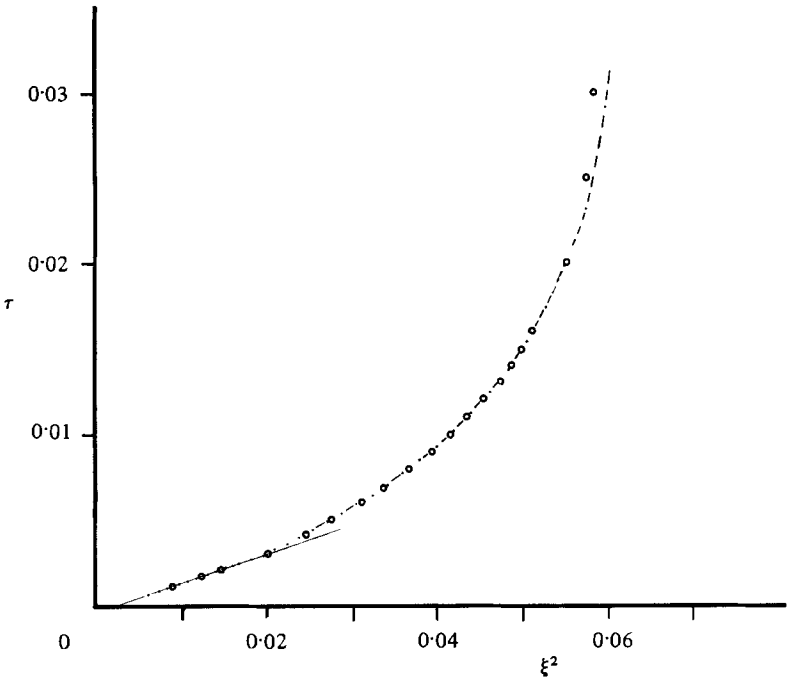

FIGURE 4. τ versus ξ^2: ——, equation (31); ○, modal values from figure 2 (equation (23)).

macroscopic lengthscale L that is considerably larger than the integral lengthscale of the fluctuating microscopic molecular motion and a velocity scale V. This simulation procedure is explained in appendix A and has the capability of providing quantitative results that would be virtually impossible to obtain from a physical experiment. For example, simulation values were found to concur with the values presented in figures 2(*a–c*).

An ideal comparator with which to assess the wall effect is available from Chatwin (1976). There the small-time growth of a contaminant cloud near the centre of a conduit was investigated and a procedure outlined to find $\overline{C}(x,t)$ that purposefully excluded any contribution from the solid conduit boundary. Following Chatwin (1976) a small-time asymptotic solution to the convective-diffusion equation for an initial contaminant sheet is integrated over the cross-section to provide $\overline{C}(\chi,\tau)$, where $\chi = x/2Pd$, which depends on the Péclet number $P = dU/2\kappa$. Details of this solution are given in appendix B, and points calculated from the solution (shown as open circles) on figures 5(*a–c*) indicate a skewed distribution for $\overline{C}(\chi,\tau)$ with a large upstream tail.

Two further comparators are of use here. One is the mean-concentration curve in the case of $\kappa = 0$, which is

$$\overline{C}(\chi,\tau) = \left[6P\tau\left(1-\frac{2\chi}{3\tau}\right)^{\frac{1}{2}}\right]^{-1}, \tag{32}$$

and is shown (in part) as a solid line on figures 5(*a–c*) that has $\chi = \frac{3}{2}\tau$ as asymptote. That is the location of a molecule travelling with the constant maximum flow centreline velocity. Concentration values can only occur downstream of this position by the agency of molecular diffusion. A second useful comparator is the mean concentration found using the simulation when molecular diffusion in the streamwise

direction is neglected. This second comparator shows the distribution $\bar{C}(\chi,\tau)$ that results exclusively from the advective–diffusive interaction, and is shown as a series of dots on figures 5(*a–c*). It is clear in these figures that at very small times the form of $\bar{C}$ is completely determined by direct diffusive effects, since the dots follow (32), and that dispersion makes no contribution. It is also clear (and is particularly evident in figure 5*c*) that at larger times the advective–diffusive process dominates by the fact that the dots provide the same curves as the complete simulation. This behaviour is anticipated as $\tau > P^{-\frac{1}{3}}$, and indeed the largest value of τ shown in figure 5(*c*) is approximately equal to $P^{-\frac{1}{3}}$. Generally, over the range of τ and P shown on these figures, both the dispersion and diffusion effects are important.

A comparison of the Chatwin calculation (open circles) with the full simulation (crosses) on figures 5(*a–c*) shows that at small enough times streamwise diffusion is the dominant contribution because there is little difference between the two curves. That is, the presence of the wall has virtually no impact, and this is consistent with the findings of Chatwin (1977). However, at larger times and while both diffusion and dispersion are important mechanisms, a very pronounced and increasing extension to the upstream tail of the Chatwin calculation is evident in the simulation data. This difference is the direct result of the solid boundary that is present in the simulation and excluded from the Chatwin calculation. The integral of $\bar{C}$ must equal unity, and thus this large tail causes a considerable distortion to upstream values of $\bar{C}$, which otherwise (for example if all values of $\bar{C}$ were normalized with the maximum value) would appear to be in quite reasonable agreement at downstream locations throughout figures 5(*a–c*).

A good agreement between simulated values and values calculated with Chatwin's procedure at downstream locations ($\chi \sim \frac{2}{3}\tau$) is anticipated, since there $\bar{C}$ describes contaminant that has not yet had time to reach the conduit boundaries ($\tau \ll 1$). In application, however, unless one can be sure that a contaminant cloud is not initially spread over an appreciable fraction of the flow cross-section, it is clear that the interaction of the contaminant cloud with the conduit boundary is very important even at quite small times ($\tau \sim P^{-\frac{1}{3}}$).

This work received financial support from the National Sciences and Engineering Research Council of Canada, and the authors wish to express their gratitude to S. Deakin for useful discussion on the asymptotic expansion used in §3.

Appendix A. The simulation

The motion of fluid molecules is followed as these traverse the flow cross-section in discrete steps of length $\pm L$ with speed V and for a time $\Delta t = L/V$. The values of L and V are chosen to satisfy $\kappa = \frac{1}{2}LV$. The direction of each step is determined with a random-number-generating routine on a digital computer. Each step results in displacements

$$y_{i+1} = y_i \pm L, \tag{33}$$

$$x_{i+1} = x_i + \frac{1}{V}\int_{y_i}^{y_{i+1}} u(y)\,dy \pm L, \tag{34}$$

where $u(y)$ is the mean Eulerian velocity profile. The random sense of direction (e.g. $\pm L$) in (34) is independent of that in (33). When a wall is encountered the molecule is reflected. Variables are non-dimensionalized as

$$y' = \frac{y}{d}, \quad L' = \frac{L}{d}, \quad x' = \frac{x\kappa}{d^2U}, \quad u'(y) = \frac{u(y)}{U}, \quad V' = \frac{Vd}{\kappa}, \quad t' = \frac{t\kappa}{d^2}.$$

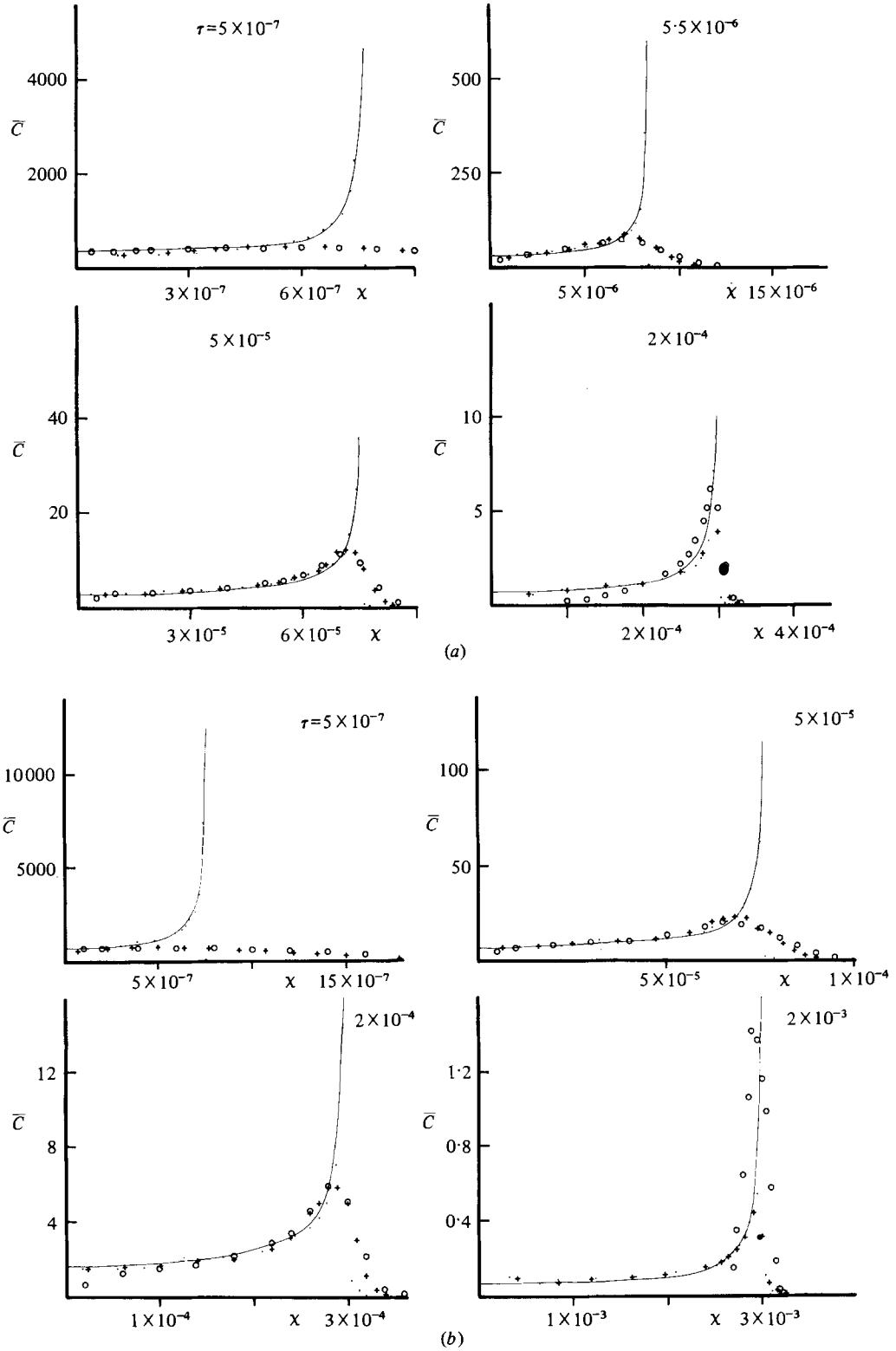

FIGURE 5(*a*, *b*). For caption see facing page.

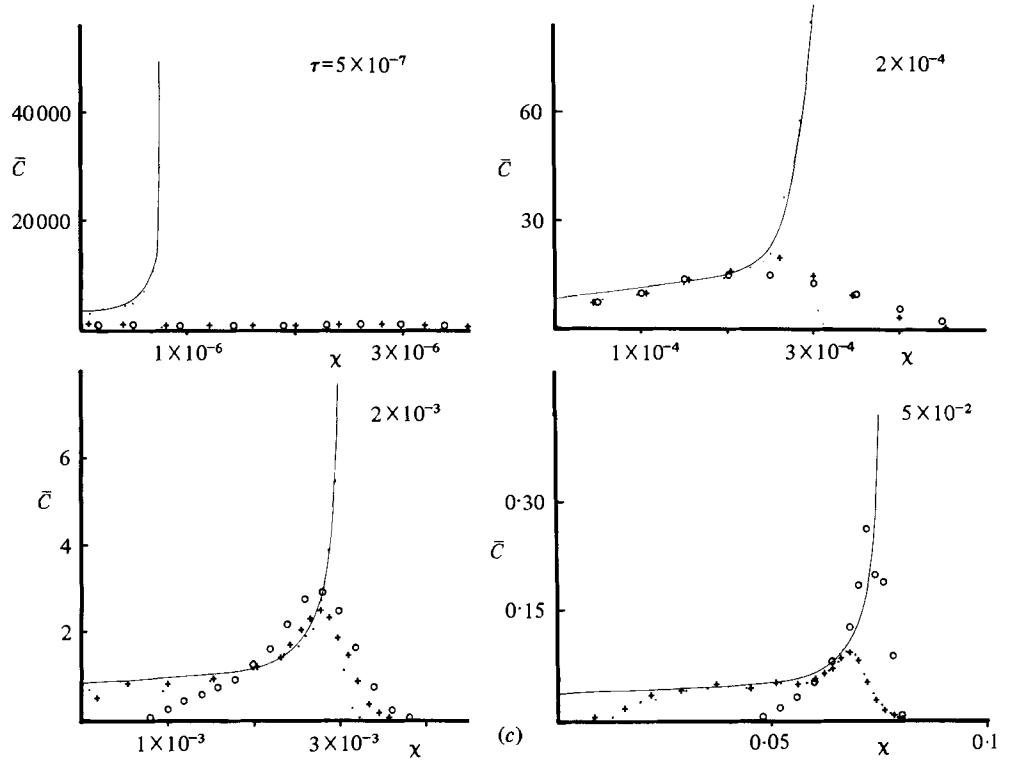

FIGURE 5. $\bar{C}$ versus χ. (*a*) $P = 1000$; (*b*) 500; (*c*) 100. ○, equation (43); +, simulation with κ; ·, simulation without κ in χ-direction; ——, equation (32).

By choosing $L' = 1/n$ then $V' = 2n$ and $\Delta t' = L'/V' = (2n^2)^{-1}$. Thus during a time interval $\Delta t'$ a molecule undergoes non-dimensional displacements

$$y'_{i+1} = y'_i \pm n^{-1}, \tag{35}$$

$$x'_{i+1} = x'_i + (2n)^{-1} \int_{y'_i}^{y'_{i+1}} u'(y')\, dy' \pm (2nP)^{-1}, \tag{36}$$

where the Péclet number $P = dU/2\kappa$ occurs explicitly only when the direct contribution of κ to longitudinal dispersion is taken into account. This is confirmed from a consideration of the convective-diffusion equation for the above non-dimensionalization, which is

$$C_{t'} + \tfrac{3}{2}(1 - \sqrt{2}\, y'^2)\, C_{x'} = \frac{1}{P^2} C_{x'x'} + C_{y'y'}. \tag{37}$$

The programme is run for a specified number of time steps $\Delta t'$, and the resultant displacements of generally 10000 molecules, which were uniformly spread on $0 \leqslant y' \leqslant 1$ at $t = 0$, are accumulated.

Appendix B. An asymptotic solution

Following Chatwin (1976) a solution to

$$C_t + \tfrac{3}{2}U\left(1 - \left(\frac{y}{a}\right)^2\right) C_x = \kappa(C_{xx} + C_{yy}), \tag{38}$$

with $C(x, y, 0) = \delta(x)\,\delta(y-y_0)$, of the form

$$C = \frac{A}{T^2}\exp\left(-(X^2+Y^2)\right)\left(1+\sum_{n=1}^{\infty} T^n\Gamma^{(n)}(X, Y)\right) \tag{39}$$

is sought, where

$$X = \frac{x-u(y_0)\,t}{2(\kappa t)^{\frac{1}{2}}}, \quad Y = \frac{y-y_0}{2(\kappa t)^{\frac{1}{2}}}, \quad T = \left(\frac{\kappa t}{a^2}\right)^{\frac{1}{2}}, \quad 2a = d$$

and $u(y)$ is the Eulerian mean-velocity profile.† With the appropriate change of variable in (38) and expansion of $u(y)$ about y_0 in a Taylor series (39) is substituted in (38) and terms with the same exponent n of T are equated to solve for $\Gamma^{(n)}(X, Y)$. The first five are found to be

$$\Gamma^{(1)} = 0, \quad \Gamma^{(2)} = -3P\zeta XY, \quad \Gamma^{(3)} = -PX(2Y^2+\tfrac{1}{2}), \tag{40a,b,c}$$

$$\Gamma^{(4)} = P^2\zeta^2[\,Y^2(\tfrac{36}{7}X-3)+\tfrac{36}{35}X-\tfrac{3}{4}], \tag{40d}$$

$$\Gamma^{(5)} = P^2[\tfrac{18}{5}\zeta X^2Y^3+\tfrac{26}{21}X^2+\tfrac{8}{3}X^2Y^2-\tfrac{231}{120}\zeta Y-\tfrac{33}{10}\zeta Y^3+\tfrac{27}{20}\zeta X^2Y+\tfrac{8}{21}Y^2+\tfrac{34}{105}], \tag{40e}$$

where $\zeta = y_0/a$ and $P = Ua/\kappa$. Defining

$$\bar{C}(X, T, \zeta) = \frac{1}{2a}\int_{-\infty}^{\infty} C\,dY, \tag{41}$$

then from (39)–(41)

$$\bar{C}(X, T, \zeta) = \frac{A\pi^{\frac{1}{2}}}{T}\exp(-X^2)\,[1-\tfrac{3}{2}PXT^3+(\tfrac{126}{35}X-\tfrac{9}{4})P^2\zeta^2T^4+(\tfrac{486}{189}X^2+\tfrac{3402}{6615})P^2T^5]. \tag{42}$$

Equation (42) is now integrated over all possible release positions y_0 on the cross-section to form

$$\begin{aligned}\bar{C}(\chi, \tau) = B\tau^{-\frac{1}{2}}\int_0^1 \exp\left[-(\tfrac{3}{2}P\tau^{\frac{1}{2}}(\tfrac{2}{3}\chi/\tau-1+\zeta^2))^2\right]\{(1-12P^2\chi\tau \\ +\tfrac{576}{7}P^4\tau^{\frac{3}{2}}\chi^2-18P^2\tau^2+\tfrac{18}{35}P^2\tau^{\frac{5}{2}}-\tfrac{1728}{7}P^4\tau^{\frac{5}{2}}\chi \\ +\tfrac{1296}{7}P^4\tau^{\frac{7}{2}})+\zeta^2(\tfrac{288}{5}P^3\tau^{\frac{3}{2}}\chi-54P^2\tau^2-\tfrac{432}{5}P^3\tau^{\frac{5}{2}} \\ +\tfrac{1728}{7}P^4\tau^{\frac{5}{2}}\chi-\tfrac{2592}{7}P^4\tau^{\frac{7}{2}})+\zeta^4(\tfrac{432}{5}P^3\tau^{\frac{5}{2}}+\tfrac{1296}{7}P^4\tau^{\frac{7}{2}})\}\,d\zeta,\end{aligned} \tag{43}$$

where B is a constant determined so that

$$\int_{-\infty}^{\infty}\bar{C}(\chi, \tau)\,d\chi = 1, \tag{44}$$

$\chi = x/2Pd$ and $\tau = t\kappa/d^2$. Equation (43) is now evaluated for specific values of ξ, P and τ using Newton–Cotes sixth-order procedure (see Fröberg 1969, p. 206).

REFERENCES

Aris, R. 1956 On the dispersion of a solute in a fluid flowing through a tube. *Proc. R. Soc. Lond.* A **235**, 67.

Bugliarello, G. & Jackson, E. 1964 Random walk study of convective diffusion. *Proc. A.S.C.E.: J. Engng Mech. Div.* **90** (EM4), 49.

Chandrasekhar, S. 1943 Stochastic problems in physics and astronomy. *Rev. Mod. Phys.* **15**, 1.

† A more complex expansion using three-dimensional Hermite polynomials and which could be made to satisfy the zero-flux condition at the wall as outlined in Chatwin & Sullivan (1981) could be used here. This is unwarranted for this purpose, which is to generate a comparator that completely excludes the wall effect.

CHATWIN, P. C. 1970 The approach to normality of the concentration distribution in solvent flowing along a straight pipe. *J. Fluid Mech.* **43**, 321.

CHATWIN, P. C. 1971 On the interpretation of some longitudinal dispersion experiments. *J. Fluid Mech.* **48**, 689.

CHATWIN, P. C. 1976 The initial dispersion of contaminant in Poiseuille flow and the smoothing of the snout. *J. Fluid Mech.* **77**, 593.

CHATWIN, P. C. 1977 The initial development of longitudinal dispersion in straight tubes. *J. Fluid Mech.* **80**, 33.

CHATWIN, P. C. & SULLIVAN, P. J. 1981 Diffusion in flows with variable diffusivity. In *Proc. A.S.M.E./A.S.C.E. Mech. Conf., Boulder, Colorado.*

CHATWIN, P. C. & SULLIVAN, P. J. 1982 The effects of aspect ratio on longitudinal diffusivity in rectangular channels. *J. Fluid Mech.* **120**, 347–358.

CSANADY, G. T. 1973 *Turbulent Diffusion in the Environment.* Reidel.

DEWEY, R. & SULLIVAN, P. J. 1977 The asymptotic stage of longitudinal turbulent dispersion within a tube. *J. Fluid Mech.* **80**, 293.

DEWEY, R. J. & SULLIVAN, P. J. 1979*a* Longitudinal dispersion in flows that are homogeneous in the streamwise direction. *Z. angew. Math. Phys.* **30**, 601.

DEWEY, R. & SULLIVAN, P. J. 1979*b* Diffusion in diverging and converging channels. *Trans. C.S.M.E.* **5**, 135.

FRÖBERG, C. N. 1969 *Introduction to Numerical Analysis*, 2nd edn. Addison-Wesley.

GILL, W. N. & SANKARASUBRAMANIAN, R. 1970 Exact analysis of unsteady convective diffusion. *Proc. R. Soc. Lond.* A **316**, 341.

LIGHTHILL, M. J. 1966 Initial development of diffusion in Poiseuille flow. *J. Inst. Math. Applics* **2**, 97.

LUMLEY, J. L. 1972 Application of central limit theorems to turbulence problems. In *Statistical Models and Turbulence* (ed. M. Rosenblatt & C. Van Atta). Lecture Notes in Physics vol. 12, p. 1. Springer.

SAFFMAN, P. G. 1960 On the effect of the molecular diffusivity in turbulent diffusion. *J. Fluid Mech.* **8**, 273.

SMITH, R. 1981 A delay-diffusion description for contaminant dispersion. *J. Fluid Mech.* **105**, 469.

SMITH, R. 1982 Gaussian approximation for contaminant dispersion. *Q. J. Mech. Appl. Math.* **35**, 345.

SULLIVAN, P. J. 1971*a* Some data on the distance-neighbour function for relative diffusion. *J. Fluid Mech.* **47**, 601.

SULLIVAN, P. J. 1971*b* Longitudinal dispersion within a two-dimensional turbulent shear flow. *J. Fluid Mech.* **49**, 551.

TAYLOR, G. I. 1921 Diffusion by continuous movements. *Proc. Lond. Math. Soc.* **20**, 196.

TAYLOR, G. I. 1953 Dispersion of soluble matter in solvent flowing slowly through a tube. *Proc. R. Soc. Lond.* A **219**, 186.